Size and shape affects the antimicrobial activity of quaternized nanoparticles

Inam, Maria; Foster, Jeffrey C.; Gao, Jingyi; Hong, Yuanxiu; Du, Jianzhong; Dove, Andrew P.; O'Reilly, Rachel K.

DOI:
10.1002/pola.29195

Size and Shape Affects the Antimicrobial Activity of Quaternized Nanoparticles

Maria Inam,[1] Jeffrey C. Foster,[2] Jingyi Gao,[3] Yuanxiu Hong,[3] Jianzhong Du,[3] Andrew P. Dove,[2] Rachel K. O'Reilly[2]

[1]University of Warwick, Department of Chemistry, Coventry, CV4 7AL, United Kingdom
[2]University of Birmingham, School of Chemistry, Edgbaston, Birmingham, B15 2TT, United Kingdom
[3]Tongji University, School of Materials Science and Engineering, etc.

Correspondence to: Rachel K. O'Reilly (R.OReilly@bham.ac.uk) or Andrew P. Dove (A.Dove@bham.ac.uk)

ABSTRACT: The size and shape of nanoparticles has been demonstrated to affect their biodistribution, cellular uptake, and biological activity. To explore these effects on antibacterial activity, crystallization driven self-assembly (CDSA) was utilized to prepare nanoparticles with spherical or platelet morphologies of different sizes. We report that small 2D platelets (< 1 μm) exhibited greater antibacterial activity than larger 2D platelets (ca. 4 μm), their corresponding spherical constructs, and unassembled polymer chains. We also observed that the size, shape, and membrane structure of the bacteria were critical in determining the biological activity of the nanoparticles, with platelets whose size was on the same order of magnitude as the bacteria exhibiting the greatest antibacterial activity.

KEYWORDS: self-assembly, polymers, platelets, biological activity, size effects

Infectious diseases induced by bacteria affect millions of people worldwide. Although many generations of antibiotics have been developed, the continuous rise in bacterial drug resistance is becoming an increasing concern for public health, driving the need for new antibacterial therapies. Several promising antibacterial agents have emerged, including silver particles,[1] metal oxide nanopartiles,[2] antimicrobial peptides,[3] and organic nanostructures.[4] Recently, two-dimensional (2D) graphene materials have been considered as antibacterials, where direct contact of their sharp edges with bacterial membranes has been proposed to induce physical damage to bacteria.[5, 6]

Using simulations, previous studies have theorised that the shape of such nanomaterials is crucial to their interaction with the lipid bilayer in translocation processes,[7] which is believed to be directly related to antimicrobial activity. It was suggested that the ability of a nanoparticle to penetrate across a membrane is determined by the contact area between the particle and the membrane and the local curvature of the particle at the contact point.[7] Additional parameters, such as rotation of the particle, are also important for non-spherical constructs, complicating the penetration process even further.[8]

Cationic compounds are well-known as potential candidates for antibacterial agents, including surfactants,[9, 10] peptides,[11, 12] and cationic polymers.[13] In particular, self-assembled cationic polymer nanostructures exhibit an increase in charge density, allowing for easier membrane rupture and thus improved antibacterial activity.[14] These nanoparticles also allow opportunities to improve antimicrobial properties further by modification of variables which have been considered to affect antimicrobial activity, including chemistry, size, shape and surface charge of the particle.[15, 16] For example, Jang and co-workers found that smaller spherical particles exhibited higher antibacterial activity than larger spherical particles due to an increase in surface area.[17] Notably,

however, Chen and co-workers compared the antibacterial activity of polymer nano-objects with sheet-like, cylindrical and spherical shapes and found no significant difference in antibacterial performance across the series.[18] One challenge, which is highlighted by these previous works, is that conventional self-assembly methods afford cylinders of high length dispersity and also sheets of undefined size and shape, this can limit the ability to interpret morphology and size effects. Hence, the effect of size of such non-spherical particles on antibacterial activity is much less investigated.

Quaternized PDMAEMA has previously been considered as a promising antimicrobial agent[19, 20] and has been immobilized on the surface of various shaped substrates including spherical[21] and cylindrical-shaped[22, 23] structures to show antibacterial activity. However, the combined effect of particle shape and size on antibacterial activity is yet to be fully understood. Herein, we report the

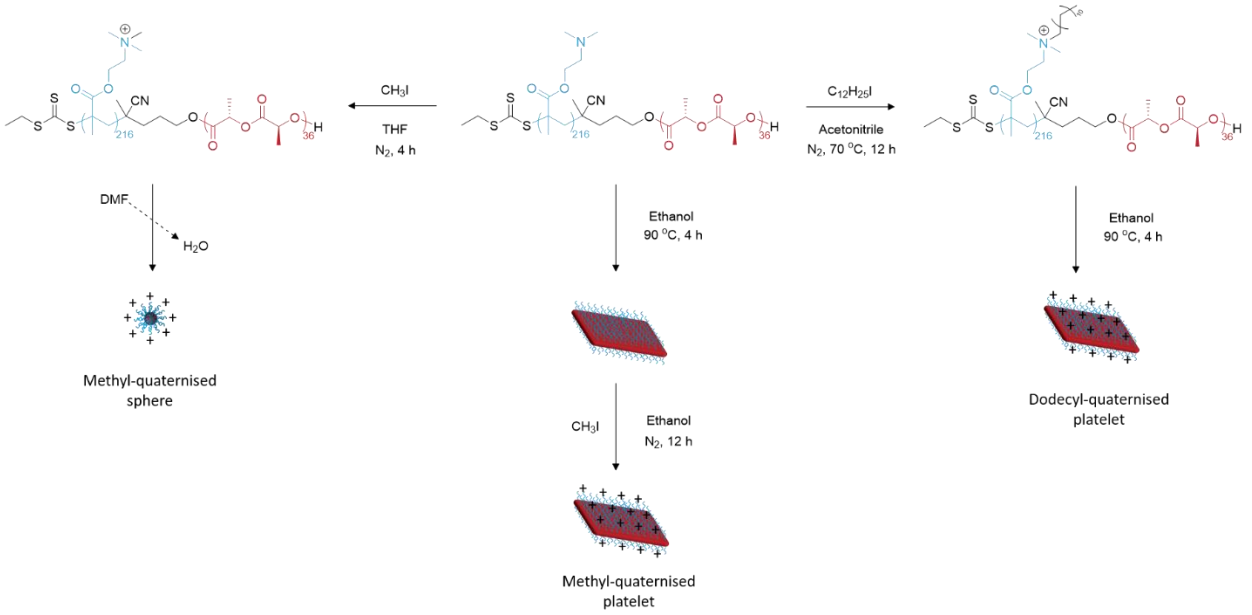

Scheme 1. Preparation of quaternised $PLLA_{36}$-*b*-$PDMAEMA_{216}$ cationic spheres and crystalline platelets.

antibacterial activity of quaternized poly(L-lactide)-*block*-poly(dimethylaminoethyl methacrylate) (PLLA-*b*-PDMAEMA) block copolymers assembled into spherical particles and diamond-shaped platelets of 2 different sizes using a crystalline driven self-assembly (CDSA) approach.

Based on synthetic methods that we recently established,[24, 25] a $PLLA_{36}$-*b*-$PDMAEMA_{216}$ diblock copolymer with a crystallizable PLLA block and a stabilizing PDMAEMA bock was synthesised *via* ring-opening polymerisation (ROP) of L-lactide followed by reversible addition-fragmentation chain transfer (RAFT) polymerization of DMAEMA from a dual-functional chain transfer agent and ROP initiator (Scheme 1, Table S1). ^{1}H NMR spectroscopic analysis was used to confirm the degree of polymerization (Fig. S1), and a narrow dispersity (1.26) of the polymer and monomodal distribution was confirmed by SEC refractive index (RI) analysis, with good overlap of the UV (λ = 309 nm) trace showing retention of the RAFT CTA end group (Fig. S2).

A series of cationically-charged nanostructures were prepared using both CDSA and conventional self-assembly (Scheme 1). Diamond-shaped platelets were prepared by heating the polymer (at 5 mg mL^{-1} in ethanol) in a sealed vial for 4 h before cooling to room temperature and ageing for one day. Semi-crystalline platelets *ca.* 600 ± 70 nm in length (on the longest axis) were formed as confirmed by transmission electron microscopy (TEM) and wide-

angle X-ray diffraction (WAXD) analysis (Figure 1a and Figure S3, respectively), with a thickness of *ca.* 12 nm as measured by atomic force microscopy (AFM, Figure S4). We have previously shown that increasing the solubility of the unimer in the assembly solvent allows for access to larger diamonds with no change in their thickness.[26] Hence, diamond-shaped platelets of *ca.* 3700 ± 200 nm (long axis) were prepared using a 88:12 ethanol/THF solution following a similar assembly procedure (Figure 1d). We shall refer to the 0.6 µM platelets as small plates, and the 3.7 µM plates as large platelets. Quantitative methyl-quaternization of these two platelets sizes was achieved using CH_3I post-assembly, as confirmed by ^1H NMR spectroscopy (Figure S5). TEM analysis confirmed no significant difference in the dimensions or dispersity of the platelets before and after modification, as previously reported (Figures 1b and 1e).[25, 26]

We also explored the dodecyl-quaterization of the constructs, as this modification has been reported to have improved activity given the more hydrophobic nature of the modification.[27] However, due to the harsher conditions required for the dodecyl-quaternization, this modification was carried out on the polymer prior to assembly (Figure S6). Again, ^1H NMR spectroscopy confirmed quantitative quaternization. Despite this change in parent polymer properties, the CDSA of the dodecyl quaternized polymer resulted in diamond-shaped small and large platelets of comparable size to those prepared from the non-modified polymer (Figures 1c and 1f). As a control nanostructure, the methyl-quaternized

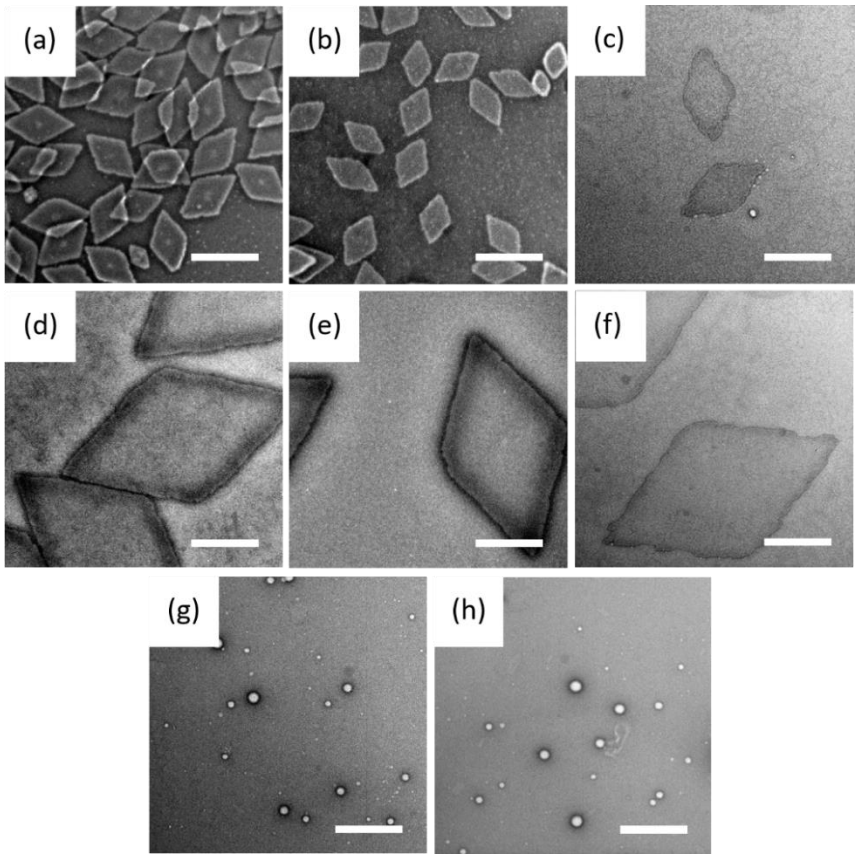

Figure 1. TEM micrographs (stained with uranyl acetate) of $PLLA_{36}$-*b*-$PDMAEMA_{216}$ small platelets (a) unquaternized, (b) quaternized with a methyl group and (c) quaternized with a dodecyl group; $PLLA_{36}$-*b*-$PDMAEMA_{216}$ large platelets (d) unquaternized, (e) quaternized with a methyl group and (f) quaternized with a dodecyl group; $PLLA_{36}$-*b*-$PDMAEMA_{216}$ spheres (g) unquaternized and (e) quaternized with a methyl group. Scale bar = 1 µm.

polymer was self-assembled using conventional solvent-switch methods to afford a spherical particle. The spherical morphology was confirmed by TEM analysis (Figures 1g and 1h for un-quaternized and quaternized, respectively), and a diameter of 136 ± 35 nm was measured by dynamic light scattering (DLS) analysis. Positive zeta potential values were measured for all of the quaternized constructs, confirming cationic charge was present on all particle surfaces (Table S2).

Given the previous work on the antibacterial testing of PDMAEMA we first explored the activity relative to *S. aureus*. Antibacterial testing was carried out by applying a set of pre-determined concentrations (62.5 µg/mL to 1000 µg/mL) of platelet dispersions in water onto the surface of a glass petri dish, followed by slow evaporation of water. A bacterial solution of *S. aureus* was then added to petri dishes (4 repeats) and incubated for 2 h.

As expected, dense bacterial colonies were observed in the control sample without any platelet additives (Figure S6). When the large platelets were used, a decrease in the number of bacterial colonies were observed above a concentration of 125 µg mL^{-1} of platelets, with no bacterial growth observed for a platelet concentration of 1000 µg mL^{-1}. When small platelets were used, much lower particle

Table 1. MIC test with methyl-quaternized nanostructures and polymers.

Bacteria property				MIC (µg mL^{-1})			
Bacteria[a]	+ or – [b]	Shape	Size (µm)	Small platelets	Large platelets	Spheres	Homopolymer
S. aureus	+	Sphere	0.5	64	128	128	256
M. luteus	+	Sphere	1	128	>512	256	>512
N. gonorrhoeae	–	Sphere	1	256	256	256	256
P. aeruginosa	–	Rod	0.5	128	256	256	>512
E. coli	–	Rod	1.5	>512	>512	>512	>512
L. monocytogenes	+	Rod	1.5	128	128	128	256
B. subtilis	+	Rod	2	128	128	128	128

[a]*Bacteria abbreviations: Staphylococcus aureus, Escherichia coli, Listeria monocytogenes, Bacillus subtilis, Micrococcus luteus, Neisseria gonorrhoeae, Pseudomonas aeruginosa.* [b] *+ or – indicates gram-positive and gram-negative bacteria, respectively.*

concentrations were needed to inhibit bacterial growth, with a decrease in bacterial colonies relative to the control sample observed as low as 62.5 µg mL^{-1} of platelets and no bacterial growth observed at 500 µg mL^{-1}.

To quantify the antibacterial activity, the killing efficacy was calculated quantitatively by determining the antibacterial rate and log reduction values from optical density (OD) mesurements.[28, 29] As shown in Figure S8 and Table S3, at a nanostructure concentration of 250 µg mL^{-1} of small or large platelets, the Log reduction values obtained were 2.63 and 1.42, respectively, confirming the greater antibacterial activity for the smaller platelets. Indeed, less than half the concentration of small platelets was needed to exhibit the same antibacterial activity as the large platelets. Indeed, this trend in greater activity of small platelets was consistent across all concentrations studied (Figure S7, Table S3).

As a control, the antibacterial activity of spherical particles prepared from the same polymer were also examined (Figure S8). Across the concentration series (62.5 µg/mL, to 2500 µg/mL), a lower antibacterial activity was measured for spheres in comparison to the small platelets, as calculated by antibacterial rate and log reduction values (Fig. S7 and Table S3), although MICs did not follow this trend. However, a higher antibacterial activity was observed for spheres in comparison to the larger platelets, showing that not only morphology, but also the size of the assembly plays a key role in determining antibacterial activity. While the mechanism of action of the platelets against bacterial cells is currently unclear, it is possible that the high charge density and compact size of the small platelets allows for tighter contacts with the bacteria in solution. A corresponding PDMAEMA homopolymer was also used as an additional control, which, as expected, exhibited a much lower antibacterial activity. Even at a

concentration of 5000 μg mL^{-1} the homopolymer was unable to completely inhibit bacterial growth.

We also tested the antibacterial activity of the constructs against *E. coli*. As shown in Table 1, all of the nanostructures were found to be ineffective in limiting the growth of *E. coli,* with MICs of > 512 μg mL^{-1}. Given that E. coli has a different size, shape, and outer membrane structure than *S. aureus* (and is also Gram-negative rather than Gram-positive) we decided to explore the MIC of these constructs across a range of different bacteria (Table 1). Initially, the antimicrobial activity of the quaternized particles against *M. luteus*, a Gram-positive spherical bacteria of *ca.* 1 μm in diameter, followed a trend similar to that the *S. aureus* sample (which is also a spherical bacterium but only around 0.5 μm in diameter), with small platelets exhibiting the lowest MIC. As observed for *E. coli*, no notable difference in MIC between the different constructs was observed with *N. gonorrhoeae,* a Gram-negative bacterium of similar shape and size to *M. luteus*.

To further elucidate the impact of bacterial size and shape on the effectiveness of the quaternized particles, MIC tests were conducted using *P. aeruginosa,* a Gram-negative bacteria of rod-shape similar to that of *E. coli* but of a size similar to *S. aureus*. As shown in Table 1, a lower MIC value was obtained when treating *P. aeruginosa* with small platelets in comparison to the large platelets and spheres. This suggested that effectiveness of the constructs is highest when the size of the construct is similar to the bacteria size. To further expand this study, two Gram-positive bacteria *B. subtilis* and *L. monocytogenes*, with larger sizes and which are rod-shaped were also tested. However, the antibacterial activity of the range of different nanostructures against these 2 bacteria did not appear to vary as a function of particle size or shape, which we propose is as a result of the mismatch of size the bacteria and construct.

Table 2. MIC test with dodecyl-quaternized polymers.

Bacteria[a]	MIC (μg mL^{-1})	
	Small platelets	Large platelets
E. coli N43	64	64
E. coli D22	64	256
E. coli NCTC	64	128

[a]*Bacteria abbreviations: Escherichia coli*

Previous work has demonstrated that increasing the length of the alkyl quaternized chain improves the antibacterial activity of polymeric materials.[27, 30] This dependence of activity on alkyl chain length has been rationalized in terms of their differential adsorption and cell membrane insertion, which is especially important in Gram-negative bacteria which has a much thicker membrane and hence is more hydrophobic. Hence, the effect of the quaternary ammonium structure on antibacterial activity was investigated by preparing small and large diamond-shaped platelets with a more hydrophobic dodecyl alkyl ammonium group. This was explored against several common strains of *E. coli*. As shown in Table 2, smaller platelets demonstrated a much lower MIC value for 2 of the strains, *E. coli* D22 and *E. coli* NCTC. However, an equivalent and MIC value for both platelet sizes was found for *E. coli N43*; however, this bacterial strain is known to be hypersensitive to drugs, which may explain this low value. As expected, these values were significantly lower than those obtained using the particles quaternized with methyl iodide, however, the trends in relation to particle size were still observed.

In summary, we have compared the antibacterial activity of quaternized $PLLA_{36}$-*b*-$PDMAEMA_{216}$ small and large platelet structures, where it was found that, in general, small platelets (ca. 0.6 μM in size) exhibited higher antibacterial activity than large platelets or spherical structures. This trend appeared to be consistent for bacteria with different shapes, sizes, and outer membrane structures. We envision that these findings could inform the design of future antibacterial formulations; however, further studies are warranted to elucidate the mechanism of action of quaternized platelets against bacterial cells.

ACKNOWLEDGEMENTS

The authors would like to thank the ERC (), EPSRC Royal Society and NSFC (21674081) for funding.

REFERENCES AND NOTES

1. G. A. Martínez-Castañón, N. Niño-Martínez, F. Martínez-Gutierrez, J. R. Martínez-Mendoza and F. Ruiz, *J. Nanopart. Res.*, 2008, **10**, 1343-1348.
2. K. R. Raghupathi, R. T. Koodali and A. C. Manna, *Langmuir*, 2011, **27**, 4020-4028.
3. M. Zasloff, *Nature*, 2002, **415**, 389-395.
4. E.-R. Kenawy, S. D. Worley and R. Broughton, *Biomacromolecules*, 2007, **8**, 1359-1384.
5. X. Zou, L. Zhang, Z. Wang and Y. Luo, *J. Am. Chem. Soc*, 2016, **138**, 2064-2077.
6. H. Ji, H. Sun and X. Qu, *Adv. Drug Deliv. Rev.*, 2016, **105**, 176-189.
7. K. Yang and Y.-Q. Ma, *Nature Nanotechnol.*, 2010, **5**, 579-583.
8. H. Sun, Y. Hong, Y. Xi, Y. Zou, J. Gao and J. Du, *Biomacromolecules*, 2018, **19**, 1701-1720.
9. T. Hamouda, A. Myc, B. Donovan, A. Y. Shih, J. D. Reuter and J. R. Baker, *Microbiol. Res.*, 2001, **156**, 1-7.
10. J. M. Hickman-Davis, F. C. Fang, C. Nathan, V. L. Shepherd, D. R. Voelker and J. R. Wright, *Am. J. Physiol. Lung Cell Mol. Physiol.*, 2001, **281**, L517-L523.
11. D. J. Davidson, A. J. Currie, G. S. D. Reid, D. M. E. Bowdish, K. L. MacDonald, R. C. Ma, R. E. W. Hancock and D. P. Speert, *J. Immunol.*, 2004, **172**, 1146-1156.
12. C. H. Park, E. V. Valore, A. J. Waring and T. Ganz, *J. Bio. Chem.*, 2001, **276**, 7806-7810.
13. A. Muñoz-Bonilla and M. Fernández-García, *Prog. Polym. Sci.*, 2012, **37**, 281-339.
14. L. Liu, K. Xu, H. Wang, P. J. Tan, W. Fan, S. S. Venkatraman, L. Li and Y.-Y. Yang, *Nature Nanotechnol.*, 2009, **4**, 457-463.
15. K. Fukushima, J. P. K. Tan, P. A. Korevaar, Y. Y. Yang, J. Pitera, A. Nelson, H. Maune, D. J. Coady, J. E. Frommer, A. C. Engler, Y. Huang, K. Xu, Z. Ji, Y. Qiao, W. Fan, L. Li, N. Wiradharma, E. W. Meijer and J. L. Hedrick, *ACS Nano*, 2012, **6**, 9191-9199.
16. H. Murata, R. R. Koepsel, K. Matyjaszewski and A. J. Russell, *Biomaterials*, 2007, **28**, 4870-4879.
17. J. Song, H. Kong and J. Jang, *Chem. Commun.*, 2009, 5418-5420.
18. D. Yao, Y. Guo, S. Chen, J. Tang and Y. Chen, *Polymer*, 2013, **54**, 3485-3491.
19. L.-A. B. Rawlinson, J. P. O'Gara, D. S. Jones and D. J. Brayden, *J. Med. Microbiol.*, 2011, **60**, 968-976.
20. G. Lu, D. Wu and R. Fu, *React. Funct. Polym.*, 2007, **67**, 355-366.
21. Z. Cheng, X. Zhu, Z. Shi, K. Neoh and E. Kang, *Ind. Eng. Chem. Res.*, 2005, **44**, 7098-7104.
22. H. Wang, L. Wang, P. Zhang, L. Yuan, Q. Yu and H. Chen, *Colloids Surf. B Biointerfaces*, 2011, **83**, 355-359.
23. A. E. Özçam, K. E. Roskov, R. J. Spontak and J. Genzer, *J. Mater. Chem.*, 2012, **22**, 5855-5864.
24. N. Petzetakis, A. P. Dove and R. K. O'Reilly, *Chem. Sci.*, 2011, **2**, 955-960.
25. M. Inam, J. R. Jones, M. M. Pérez-Madrigal, M. C. Arno, A. P. Dove and R. K. O'Reilly, *ACS Cent. Sci.*, 2018, **4**, 63-70.
26. M. Inam, G. Cambridge, A. Pitto-Barry, Z. P. Laker, N. R. Wilson, R. T. Mathers, A. P. Dove and R. K. O'Reilly, *Chem. Sci.*, 2017, **8**, 4223-4230.
27. C. Z. Chen, N. C. Beck-Tan, P. Dhurjati, T. K. van Dyk, R. A. LaRossa and S. L. Cooper, *Biomacromolecules*, 2000, **1**, 473-480.
28. C. Zhou, P. Li, X. Qi, A. R. M. Sharif, Y. F. Poon, Y. Cao, M. W. Chang, S. S. J. Leong and M. B. Chan-Park, *Biomaterials*, 2011, **32**, 2704-2712.
29. C. Zhang, Y. Zhu, C. Zhou, W. Yuan and J. Du, *Polym. Chem.*, 2013, **4**, 255-259.
30. I. Yudovin-Farber, N. Beyth, E. I. Weiss and A. J. Domb, *J. Nanopart. Res.*, 2010, **12**, 591-603.

GRAPHICAL ABSTRACT

Maria Inam, Jeffrey C. Foster, Jingyi Gao, Yuanxiu Hong, Jianzhong Du, Andrew P. Dove, Rachel K. O'Reilly

Size and Shape Affects the Antimicrobial Activity of Quaternized Nanoparticles

Crystallization driven self-assembly (CDSA) was utilized to prepare quaternized nanoparticles with spherical or platelet morphologies of different sizes to explore the effect of size and shape on their antibacterial activity. Small 2D platelets (< 1 μm) exhibited greater antibacterial activity than larger 2D platelets (ca. 4 μm), their corresponding spherical constructs, and unassembled polymer chains. This activity was dependent on the size, shape, and cell membrane structure of the bacteria.